

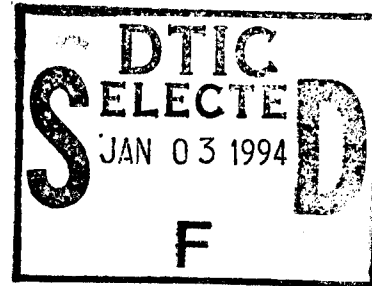
WL-TR-94-4077



Evaluation of Composite Joints

Seng C. Tan

Wright Materials Research Co.
3591 Apple Grove Dr.
Beavercreek, OH 45430



April 1994

Interim Report for Period November 1993 - April 1994

Approved for public release; distribution is unlimited

MATERIALS DIRECTORATE
WRIGHT LABORATORY
AIR FORCE MATERIEL COMMAND
WRIGHT-PATTERSON AIR FORCE BASE, OH 45433-7734

DTIC QUALITY INSPECTED 2

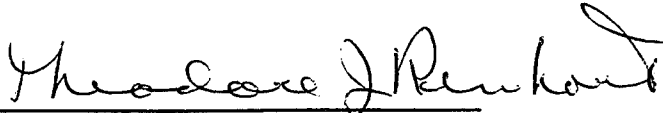
19941227 062

NOTICE

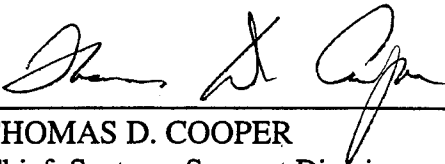
When Government drawings, specifications, or other data are used for any purpose other than in connection with a definitely Government-related procurement, the United States Government incurs no responsibility nor any obligation whatsoever. The fact that the government may have formulated, or in any way supplied the said drawings, specifications, or other data, is not to be regarded by implication or otherwise in any manner construed, as licensing the holder or any other person or corporation, or as conveying any rights or permission to manufacture, use, or sell any patented invention that may in any way be related thereto.

This report is releasable to the National Technical Information Service (NTIS). At NTIS, it will be available to the general public, including foreign nations.

This technical report has been reviewed and is approved for publication.



THEODORE J. REINHART
Chief, Materials Engineering Branch
Systems Support Division
Materials Directorate



THOMAS D. COOPER
Chief, Systems Support Division
Materials Directorate

If your address has changed, if you wish to be removed from our mailing list, or if the addressee is no longer employed by your organization, please notify WL/MLSE, Wright-Patterson AFB, OH 45433-7734 to help us maintain a current mailing list.

Copies of this report should not be returned unless return is required by security considerations, contractual obligations, or notice on a specific document.

REPORT DOCUMENTATION PAGE

Form Approved
OMB No. 0704-0188

Public reporting burden for this collection of information is estimated to average 1 hour per response, including the time for reviewing instructions, searching existing data sources, gathering and maintaining the data needed, and completing and reviewing the collection of information. Send comments regarding this burden estimate or any other aspect of this collection of information, including suggestions for reducing this burden, to Washington Headquarters Services, Directorate for Information Operations and Reports, 1215 Jefferson Davis Highway, Suite 1204, Arlington, VA 22202-4302, and to the Office of Management and Budget, Paperwork Reduction Project (0704-0188), Washington, DC 20503.

1. AGENCY USE ONLY (Leave blank)		2. REPORT DATE April 1994	3. REPORT TYPE AND DATES COVERED Interim; November 1993 - April 1994		
4. TITLE AND SUBTITLE EVALUATION OF COMPOSITE JOINTS			5. FUNDING NUMBERS C - F33615-89-C-5643 PE - 62102 PR - 2418 TA - 04 WU - 69		
6. AUTHOR(S) Seng C. Tan					
7. PERFORMING ORGANIZATION NAME(S) AND ADDRESS(ES) Wright Materials Research Co. 3591 Apple Grove Drive Beavercreek, OH 45430			8. PERFORMING ORGANIZATION REPORT NUMBER		
9. SPONSORING / MONITORING AGENCY NAME(S) AND ADDRESS(ES) Materials Directorate Wright Laboratory Air Force Materiel Command Wright-Patterson Air Force Base, OH 45433-7734			10. SPONSORING / MONITORING AGENCY REPORT NUMBER WL-TR-94-4077		
11. SUPPLEMENTARY NOTES					
12a. DISTRIBUTION / AVAILABILITY STATEMENT Approved for public release; distribution is unlimited.			12b. DISTRIBUTION CODE		
13. ABSTRACT (Maximum 200 words) A study of bolted, bonded, and bolted-bonded composite single lap joints was conducted. Graphite thermoplastic composite material (AS4/APC2) and two stacking sequences, [0,90,45,135] _{2s} and [0,0,45,135] _{2s} , were used. Five joint designs were tested; (a) bonded (FM400), (b) bolted-bonded with two bolts, (c) bolted bonded with four bolts, (d) bolted with six bolts, and (e) bolted with eight bolts. Load-deflection measurements were made and joint efficiencies computed. Failure mechanisms were determined. Peak joint efficiencies were in the 55% vicinity and occurred for the six-bolt configuration and the [0,90,45,135] _{2s} laminate. For the tests in this study, the adhesive bond failed interfacially at relatively low load levels.					
14. SUBJECT TERMS		Single Lap	Bolts	Fasteners	15. NUMBER OF PAGES
Composite Bolted		Graphite	Adhesive		16. PRICE CODE
Joints Bolted-Bonded		Thermoplastic	Failure Mechanism		
Bonded Joint Efficiency		PEEK	Shear		
17. SECURITY CLASSIFICATION OF REPORT UNCLASSIFIED	18. SECURITY CLASSIFICATION OF THIS PAGE UNCLASSIFIED	19. SECURITY CLASSIFICATION OF ABSTRACT UNCLASSIFIED	20. LIMITATION OF ABSTRACT UNLIMITED		

TABLE OF CONTENTS

<u>Section</u>		<u>Page</u>
	List of Figures	iv
	List of Tables	vi
1	Introduction	1
2	Joining Efficiency	1
3	Experimental Program	2
	3.1 Specimen Design	6
	3.2 Specimen Preparation	6
	3.3 Testing	6
4	Experimental Results and Discussion	7
	4.1 Load vs. Crosshead Displacement Relation	7
	4.2 Strength Data	10
	4.3 Failure Mechanisms	17
	4.4 Efficiency of Single-lap Joints	24
5	Conclusion	24
6	References	25

Accession For	
NTIS CRA&I	<input checked="" type="checkbox"/>
DTIC TAB	<input type="checkbox"/>
Unannounced	<input type="checkbox"/>
Justification	
By	
Distribution/	
Availability Codes	
Dist	Avail and/or Special
A-1	

LIST OF FIGURES

<u>Figure</u>		<u>Page</u>
1	A single-bolted joint specimen.	3
2	A bolted-bonded joint specimen with 2-bolt configuration.	3
3	A bolted-bonded joint specimen with 4-bolt configuration.	4
4	A bolted joint specimen with 6-bolt configuration.	4
5	A bolted joint specimen with 8-bolt configuration.	5
6	Set-up of single-lap joint specimens for tensile test.	5
7	Load-crosshead deflection relations of AS4/APC-2 [0/90/±45] _{2S} laminates with single-lap joints.	8
8	Initial region of load-crosshead deflection relations of AS4/APC-2 [0/90/±45] _{2S} laminates with single-lap joints.	8
9	Load-crosshead deflection relations of AS4/APC-2 [0 ₂ /±45] _{2S} laminates with single-lap joints.	9
10	Load-crosshead deflection relations of AS4/APC-2 [0/90/±45] _{2S} laminates with bonded joints.	11
11	Load-crosshead deflection relations of AS4/APC-2 [0 ₂ /±45] _{2S} laminates with bonded joints.	11
12	Load-crosshead deflection relations of AS4/APC-2 [0/90/±45] _{2S} laminates with bolted-bonded joints (2-bolt).	12
13	Load-crosshead deflection relations of AS4/APC-2 [0 ₂ /±45] _{2S} laminates with bolted-bonded joints (2-bolt).	12
14	Load-crosshead deflection relations of AS4/APC-2 [0/90/±45] _{2S} laminates with bolted-bonded joints (4-bolt).	13

15	Load-crosshead deflection relations of AS4/APC-2 [0 ₂ /±45] _{2s} laminates with bolted-bonded joints (4-bolt).	13
16	Load-crosshead deflection relations of AS4/APC-2 [0/90/±45] _{2s} laminates with bolted joints (6-bolt).	14
17	Load-crosshead deflection relations of AS4/APC-2 [0 ₂ /±45] _{2s} laminates with bolted joints (6-bolt).	14
18	Interfacial debonding of AS4/APC-2 specimens with bonded joints.	20
19	Failure mechanisms of an AS4/APC-2 [0/90/±45] _{2s} laminate with bolted-bonded joints (2-bolt).	20
20	Failure mechanisms of an AS4/APC-2 [0 ₂ /±45] _{2s} laminate with bolted-bonded joints (2-bolt).	21
21	Failure mechanisms of an AS4/APC-2 [0/90/±45] _{2s} laminate with bolted-bonded joints (4-bolt).	21
22	Failure mechanisms of an AS4/APC-2 [0 ₂ /±45] _{2s} laminate with bolted-bonded joints (4-bolt).	22
23	Failure mechanisms of an AS4/APC-2 [0/90/±45] _{2s} laminate with bolted joints (6-bolt).	22
24	Failure mechanisms of an AS4/APC-2 [0 ₂ /±45] _{2s} laminate with bolted joints (6-bolt).	23
25	Joining efficiency versus number of bolts for AS4/APC-2 [0/90/±45] _{2s} and [0 ₂ /±45] _{2s} laminates.	23

LIST OF TABLES

<u>Table</u>		<u>Page</u>
1	Experimental results of Gr/PEEK AS4/APC-2 coupons.	15
2	Single lap shear strength (bonded joint) of Gr/PEEK AS4/APC-2 laminates.	16
3	Strength of AS4/APC-2 specimens with bolted-bonded joints.	18
4	Experimental results of AS4/APC-2 specimens with bolted joints (6-bolt).	19
5	Experimental results of AS4/APC-2 specimens with bolted joints (8-bolt).	19

PREFACE

This report covers work performed during the period from November 1993 to April 1994. The project was supported in part by Air Force Contract F33615-89-C-5643. The work was performed by Wright Materials Research Co., under subcontract to the University of Dayton Research Institute, and administered under the direction of the System Support Division of the Wright Laboratory, Wright-Patterson Air Force Base, Ohio. Mr. Robert Urzi was the program Project Engineer. The author would like to thank Mr. R. Askins, Mr. J. Ruschau of the University of Dayton Research Institute, Mr. J. Coate and Mr. N. Ontko of WL/MLSE for assisting in preparation and testing the specimens.

1. Introduction

Joining method is a very important problem in practical applications of metal and composite structures. Although this problem has been well studied in metallic structures, many studies are needed for joining composite structures. The joining methods in polymeric composites can generally be classified into three categories: (1) bolted joints [1-8]; (2) bonded joints [9-14]; and (3) bolted-bonded joints [15]. They have all been used extensively in aircraft industry. Most of the studies that appear in the open literature are either focused on bolted joints or bonded joints. Very few of them have studied bolted-bonded joints.

Early work on bolted joints was confined to single-bolted joints and the conditions to achieve bearing strength. Recent studies have shown that structural behavior of multiple-bolted joints is very different from that of single-bolted joints. Since multiple-bolted joints have great practical applications, both theoretical and experimental study for composite structures involving mechanical joints must use multiple-bolted joints.

It is commonly believed that adhesive joints in structures can provide higher load transferring efficiency than mechanical joints. This may be true under certain material and geometric configurations. It does not represent a guaranteed relation.

The objective of this research is to evaluate the efficiency of bolted, bonded, and bolted-bonded joints in laminated composites with single-lap shear configuration and subject to tensile loading. A test program is carried out to compare the efficiency of these three different joining methods using minimum number of specimens needed. The data generated in this program can help to understand and to improve structural design involving adhesive and mechanical joints.

2. Joining Efficiency

A structure normally consists of more than one component for various reasons including manufacturing, maintenance consideration, transportation and installation, design, etc. The components are joined together using mechanical joints, bonded joints, or both. *The efficiency of the joint is defined as the load carrying capability of the structure with joints as compared to that of a single-component structure.* That is:

$$e_{ff} = \frac{\text{Failure load of a structure with joints}}{\text{Failure load of a single-component structure (same layup)}}$$

where the widths of the structures evaluated should be the same. An alternative method of evaluating the joining efficiency is to use the remote fracture strains measured by strain gauges or other techniques

$$e_{ff} = \frac{\text{Remote fracture strain of a structure with joints}}{\text{Fracture strain of a single-component structure (same layup)}}$$

One must be very careful in using the strain values to calculate the joining efficiency. If the location where the strain is measured is not sufficiently far away from the joints, cutouts or any stress concentrations, then we actually calculate the strain concentrations rather than the joining efficiency.

The definition of joining efficiency by failure load is very clear and easy to calculate. Therefore, we will use this method to evaluate the joining efficiency in this research project.

3. Experimental Program

Graphite/PEEK AS4/APC-2 unidirectional prepreg was chosen to fabricate $[0/90/\pm 45]_{2S}$ and $[0_2/\pm 45]_{2S}$ panels. Then they were sliced to the dimensions designed using diamond coated saw. Four to six replicas were fabricated and tested for each specimen configuration.

3.1 Specimen Design

The width of the specimens, with or without joints, are all 2.25 in.. Baseline specimens (coupons) are 12.7 inch in length with 2.35 inch end tabs at both ends. This leads to 8-inch gage length. Single lap joint configuration was used to evaluate the joint efficiency under tensile loading. The gauge lengths of the bolted specimens, bonded specimens, and bolted-bonded specimens are all 6 inches so that the experimental results can be plotted on the same figure for comparison.

The dimensions of the specimens with bolted joints or bolted-bonded joints are illustrated in Figures 1 through 5. The bonded areas for the specimens with bolted-bonded joints (2 bolts and 4 bolts) are all 2.25 inches by 2.25 in.. Specimens with 6 bolts or 8 bolts do not use bonded joints. Specimens with 2 bolts or 4 bolts have a region of 2.87 inches long in both

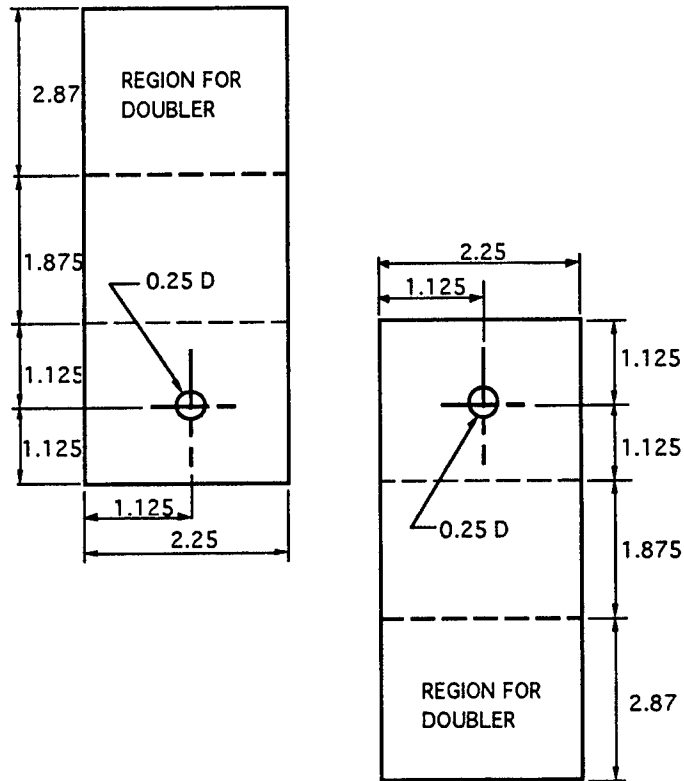


Figure 1. A single-bolted joint specimen.

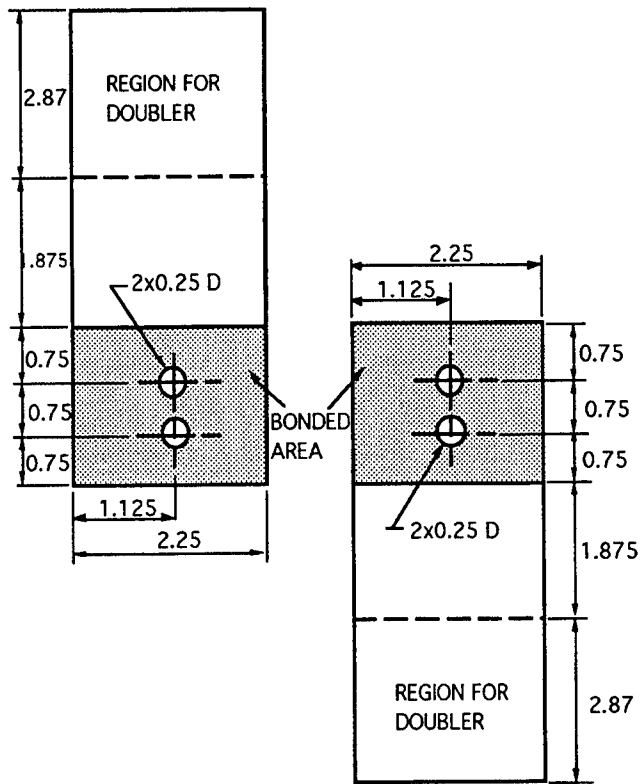


Figure 2. A bolted-bonded joint specimen with 2-bolt configuration.

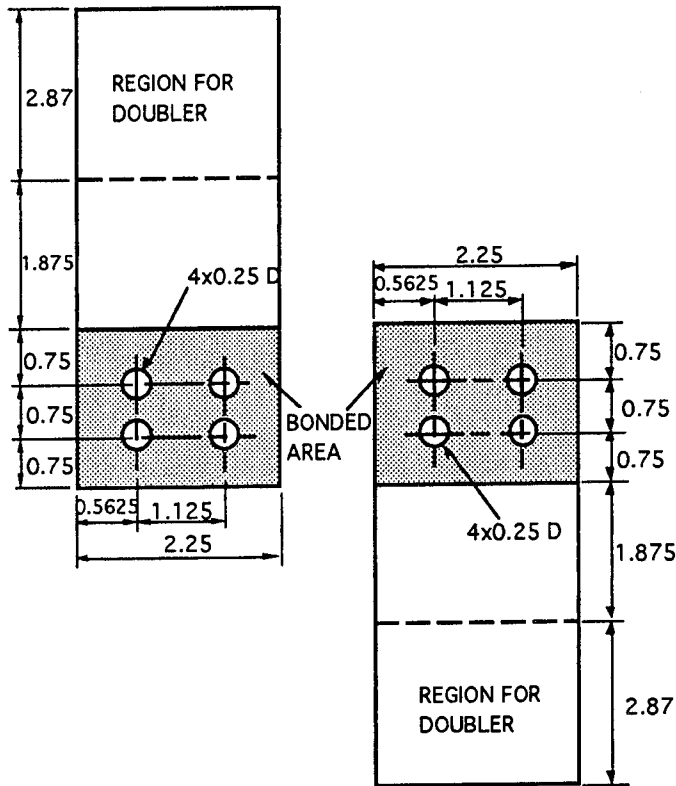


Figure 3. A bolted-bonded joint specimen with 4-bolt configuration.

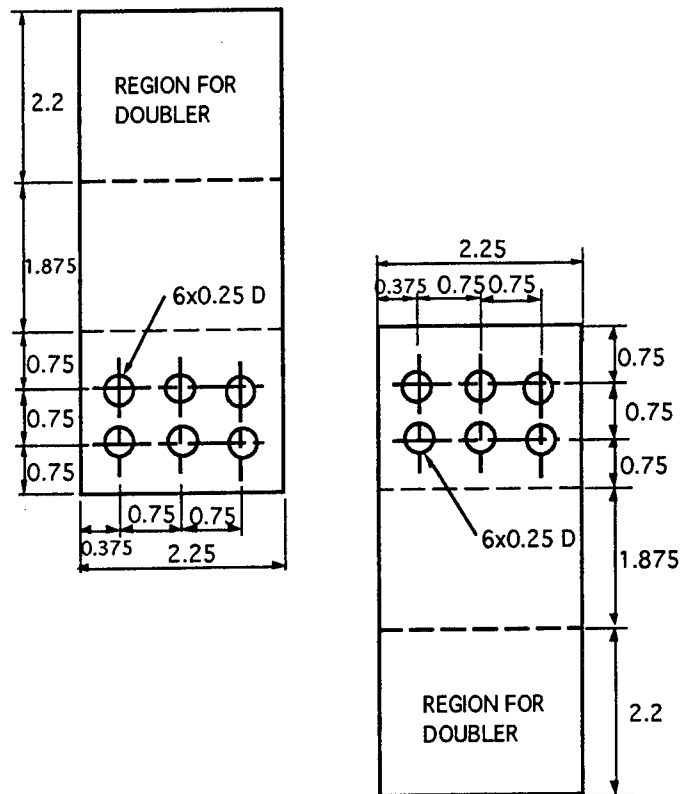


Figure 4. A bolted joint specimen with 6-bolt configuration.

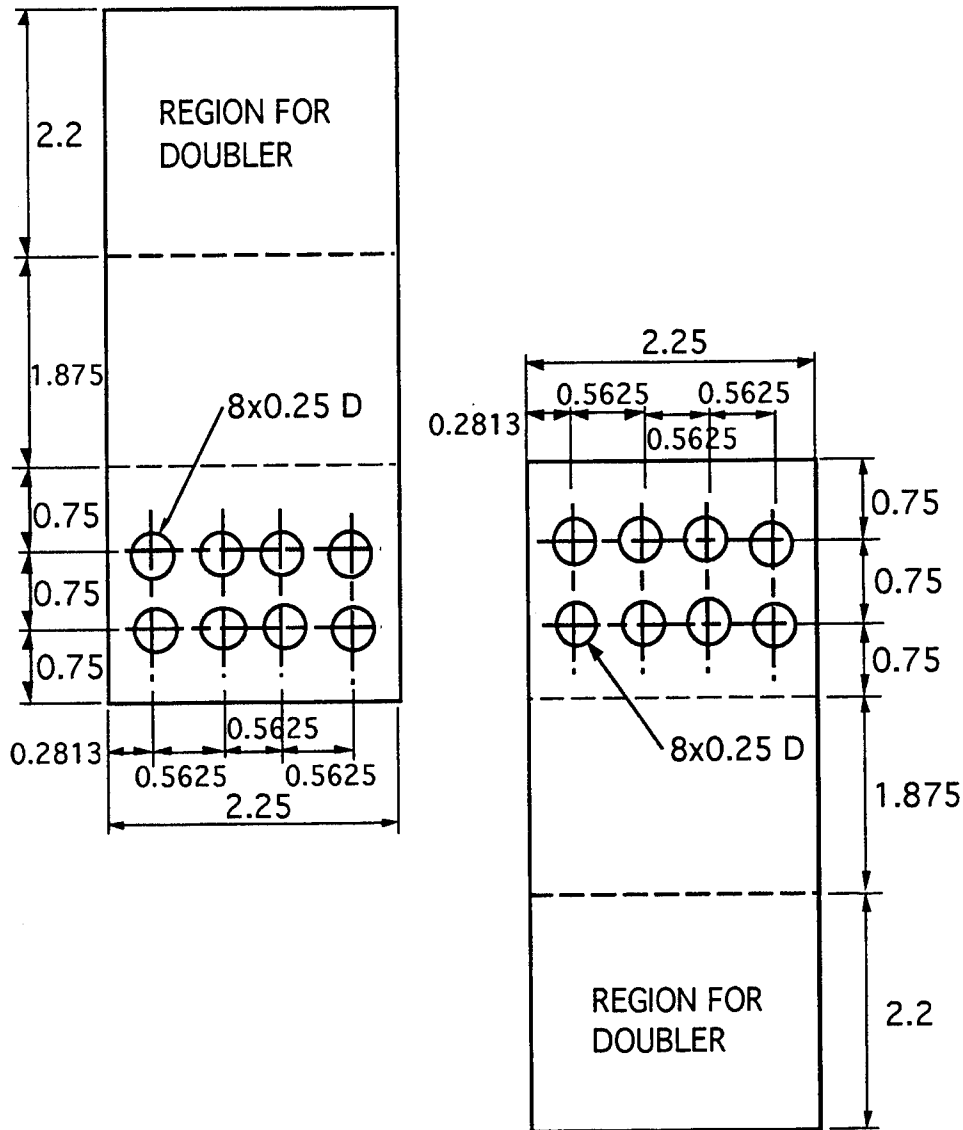


Figure 5. A bolted joint specimen with 8-bolt configuration.

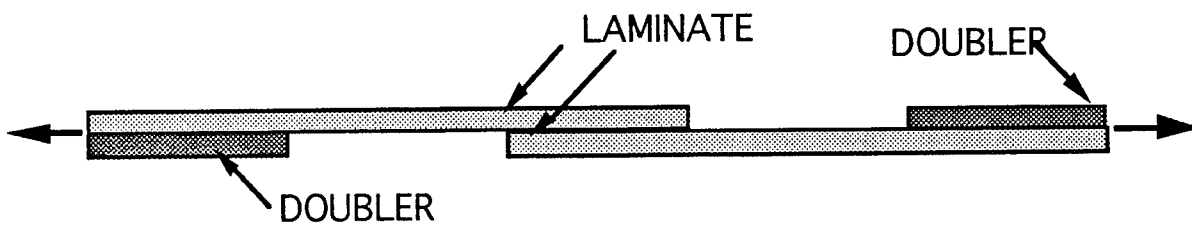


Figure 6. Set-up of single-lap joint specimens for tensile test.

ends for doublers. The distance between the overlapped joint and the doubler is 1.875 inches. The doubler regions for the specimens with 6 bolts or 8 bolts are all 2.2 inches. The bolt holes are all 0.25 inch in diameter.

The specimens with bonded joints are sketched in Figure 6. The bonded areas are all 2.25 inches by 2.25 inches. The distance between the overlapped joint and the doubler is 1.875 inches and the lengths for the doublers are 2.2 inches.

3.2 Specimen Preparation

The specimens were all cut using diamond impregnated saw, water cooled. The bolt holes were machined using a three-step procedure. First step used a 0.125-inch Carbide center drill to cut a pilot hole at a speed of 1300 RPM. Then a 15/64-inch Carbide center drill is used to enlarge the hole at a speed of 1200 RPM. Finally, we used a 0.25-inch Carbide reamer to finish the hole at a speed of 500 RPM. After the holes were cut the specimens were examined using C-SCAN to ensure that there is no damage or defects in the specimens. The diameters of the bolts were 0.25 inch that create a close-fit bolted joint. The hardness of the bolt is 20 Rockwell C. Washers were used on both sides of the specimens. The inside and outside diameters of the washer are 0.275 inch and 0.55 inch, respectively. A torque of 100 in-lb was applied to fasten all the bolts to the specimens.

The bonded surfaces of the specimens with bonded joints were roughened first using a 120-grid Silicon Carbide sandpaper. Two specimens were then grit blasted at 100-120 psi pressure. One specimen was grit blasted with the same pressure without being sanded. After the specimens were cleaned they were bonded using FM-400 adhesive (American Cyanamid). The specimens were put in an oven with bonded surfaces pressed together with approximately 35 psi, accomplished by dead weight. Heat was applied at a rate of 5° F/min.. After the oven reaches 340° F, the temperature was maintained for 1 hour. After heating, the specimens were cooled naturally to ambient temperature.

End doublers were cut from the test panel and attached to both ends of each specimen (Figure 6). This procedure ensures that the specimen has the same thickness under the machine grips and the load was applied through the center of the specimen.

3.3 Testing

Tensile loading was applied for all the specimens. The coupons were strain gauged to measure the stress-strain relation, modulus, Poisson's ratio

and fracture strength. Load versus crosshead displacement relation was measured for all specimens tested. Loading rates were all set at 0.05 in/min. Most of the specimens were loaded to ultimate failure. The load-crosshead displacement relation was digitized using data acquisition system. After the specimens were fractured, their failure mechanisms were examined and recorded.

4 Experimental Results and Discussion

The experimental results that were analyzed included load-crosshead displacement relation, ultimate strength, failure mechanisms, and the joining efficiency.

4.1 Load vs. Crosshead Displacement Relation

Since the gauge lengths of the baseline specimens (coupons) are 8 inches the crosshead deflections must be multiplied by a factor of 0.75 so that the results can be plotted on the same figure with the data with joints. Figure 7 compares the load-crosshead displacement relations of $[0/90/\pm 45]_{2s}$ coupons and specimens with bonded joints, bolted-bonded joints with 2 bolts and 4 bolts, and bolted joints with 6 bolts. All the curves exhibit somewhat nonlinearity. The result of bolted-bonded joints with 2 bolts reaches a plateau when the laminate strain (between grips) is approximately 1.17%. Figure 8 gives an exploded view of the initial portion of the load-deflection curves. All the specimens with joints have less stiffness than those of baseline specimen because of the eccentricity of the specimens. The specimens with 2 bolts and 4 bolts have the same joint stiffness initially. After we saw a sudden drop of load in the load-deflection curve, we unloaded the specimen for observation. Debonding was found in the adhesive layer. Because of the difference in load transfer mechanisms the debonding in bolted-bonded joints occurs at a lower load for 2-bolt than for 4-bolt configuration. After debonding occurs, the load is transferred through the bolts. Therefore, a bolted-bonded joint with 4-bolt has higher joint stiffness than that with 2-bolt as shown in Figure 8.

The load-deflection curves of AS4/APC-2 $[0_2/\pm 45]_{2s}$ laminates including baseline specimens, bonded joints, bolted-bonded joints with 2-bolt and 4-bolt, and bolted joints with 6-bolt are illustrated in Figure 9. Except the specimens with bonded joints and bolted-bonded joints with 2-bolt all the other specimen configurations have higher fracture loads than those of the $[0/90/\pm 45]_{2s}$ laminates as shown in Figure 8.

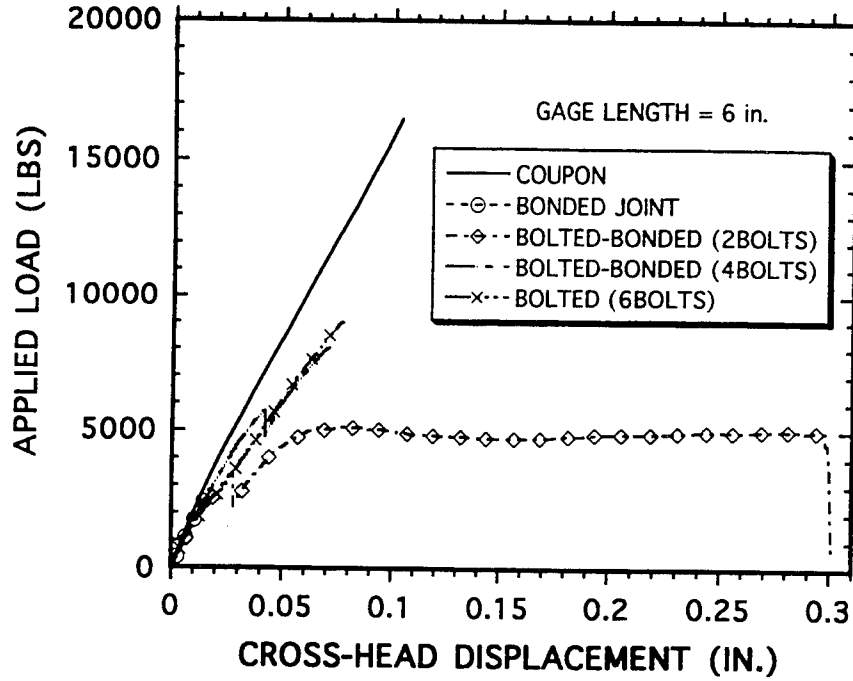


Figure 7. Load-crosshead deflection relations of AS4/APC-2 [0/90/±45]_{2s} laminates with single-lap joints.

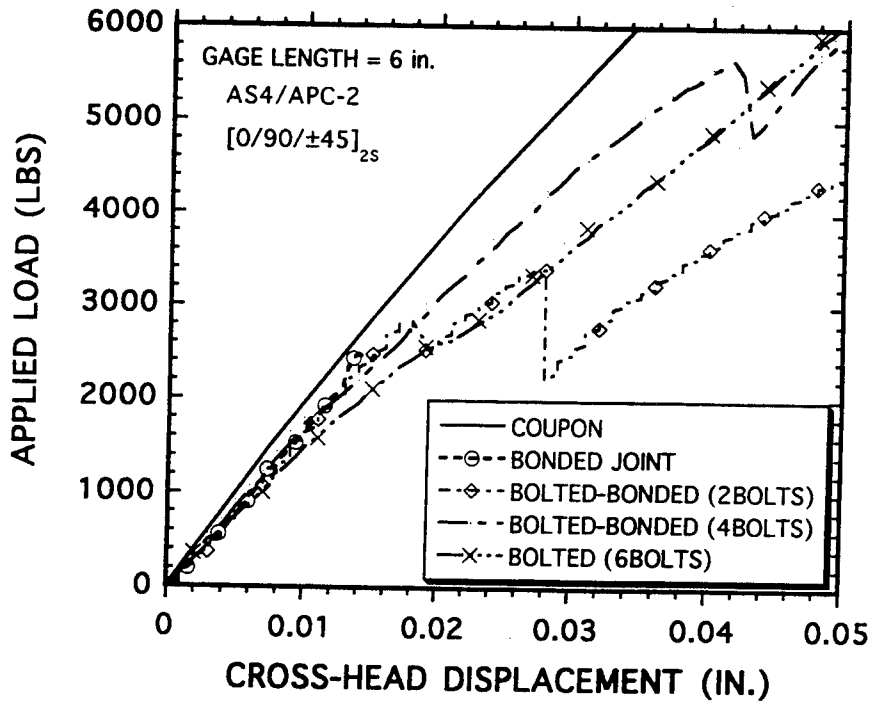


Figure 8. Initial region of load-crosshead deflection relations of AS4/APC-2 [0/90/±45]_{2s} laminates with single-lap joints.

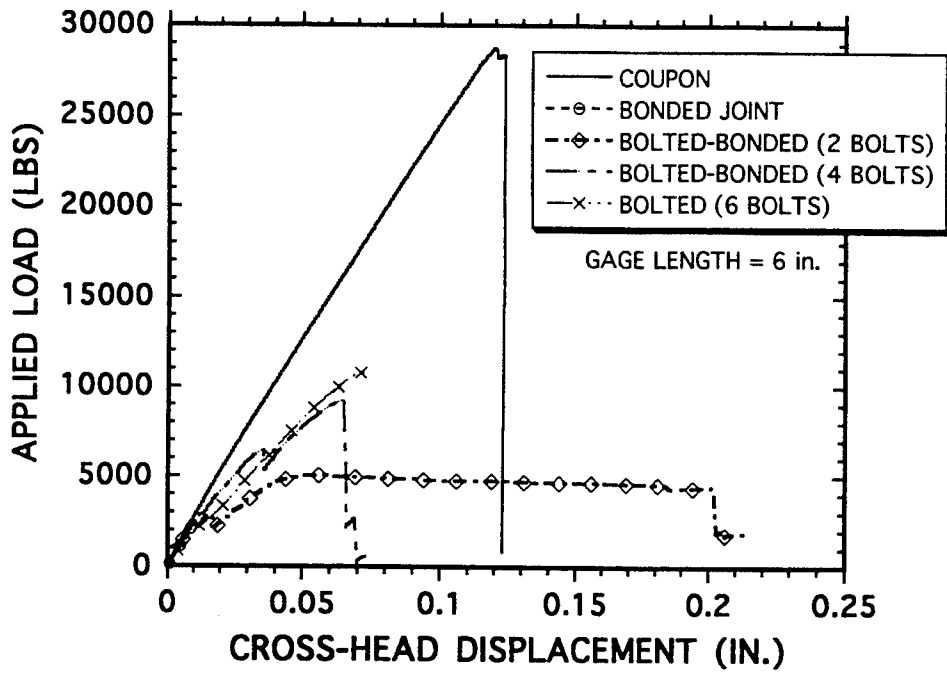


Figure 9. Load-crosshead deflection relations of AS4/APC-2 $[0_2/\pm 45]_{2S}$ laminates with single-lap joints.

In the following illustrations each figure contains the relations of load-crosshead deflections of two representative specimens. The load-deflection relations of the $[0/90/\pm 45]_{2S}$ specimens, Figure 10, with a bonded joint (single lap) are linear until just before the specimens fail. Similar behavior was observed for the $[0_2/\pm 45]_{2S}$ laminates with bonded joints, Figure 11.

The load-crosshead displacement relations of the $[0/90/\pm 45]_{2S}$ and the $[0_2/\pm 45]_{2S}$ laminates with bolted-bonded joints with 2-bolt are very similar. The first load drop of the former specimen, Figure 12, occurs at 2840 pounds, which indicates that debonding of the adhesive layer starts to occur. At 3350~3410 pounds a significant load drop appears which is caused by a complete debonding of the adhesive layer. Beyond this point the load was transferred through the bolts. At 4900~5000 pounds the curves reach a plateau that signals the initiation of bearing failure. For the $[0_2/\pm 45]_{2S}$ laminates, Figure 13, the initial and the complete debonding occurs at 2400~2800 pounds and 2800~3200 pounds, respectively.

The load-crosshead deflection relations of the $[0/90/\pm 45]_{2S}$ and the $[0_2/\pm 45]_{2S}$ laminates with bolted-bonded joints with 4-bolt are nonlinear. The load drop of these laminates occur at 5700~6206 lbs (Figure 14) and 6195~6690 pounds (Figure 15), respectively. The load drop in these two figures indicates a complete debonding of the adhesive layer. There are no distinct signals of partial debonding as those in the 2-bolt specimens. No effort was made to examine if partial debonding occurs in a progressive manner.

The load-crosshead deflection relations of the $[0/90/\pm 45]_{2S}$ (Figure 16) and the $[0_2/\pm 45]_{2S}$ (Figure 17) laminates with bolted joints (6-bolt) are linear for most part of the curves. Only a small portion at the end of the curve exhibits nonlinear behavior. The unsmoothness of the initial portions of the curves is caused by overcoming the friction between the specimen and the washer due to the applied torque.

4.2 Strength Data

The modulus, Poisson's ratio, and strength properties of the baseline specimens are listed in Table 1. The ultimate strengths of the $[0/90/\pm 45]_{2S}$ and the $[0_2/\pm 45]_{2S}$ laminates are 86.8 and 144 ksi, respectively. The bonded joint data is given in Table 2. The effects of surface preparation are reflected by the maximum load carrying capability. It is commonly believe that sanded and grit blasted surfaces result in higher joining strength. Only two specimens were tested to show the trend of joining strength in this project.

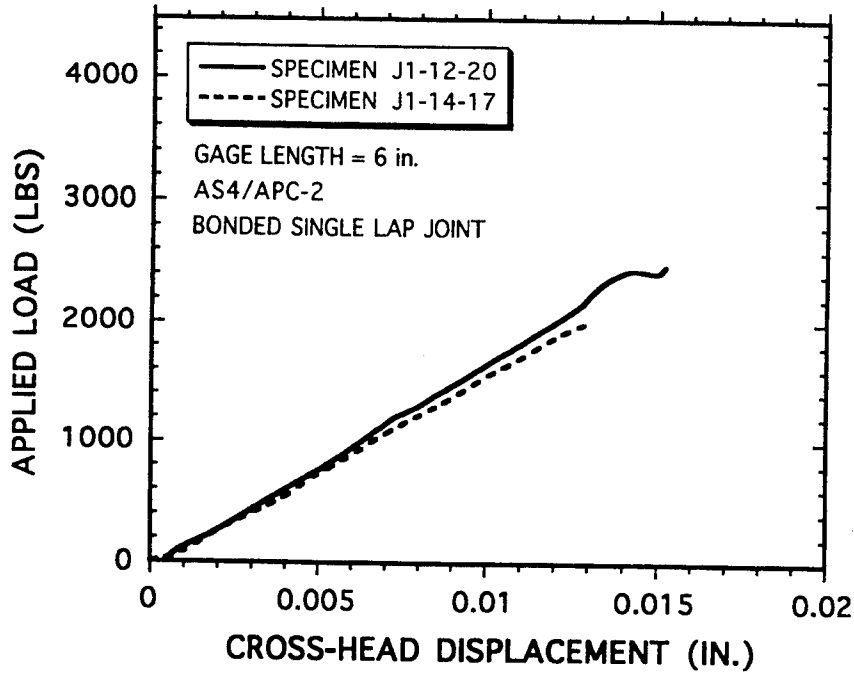


Figure 10. Load-crosshead deflection relations of AS4/APC-2 $[0/90/\pm 45]_{2s}$ laminates with bonded joints.

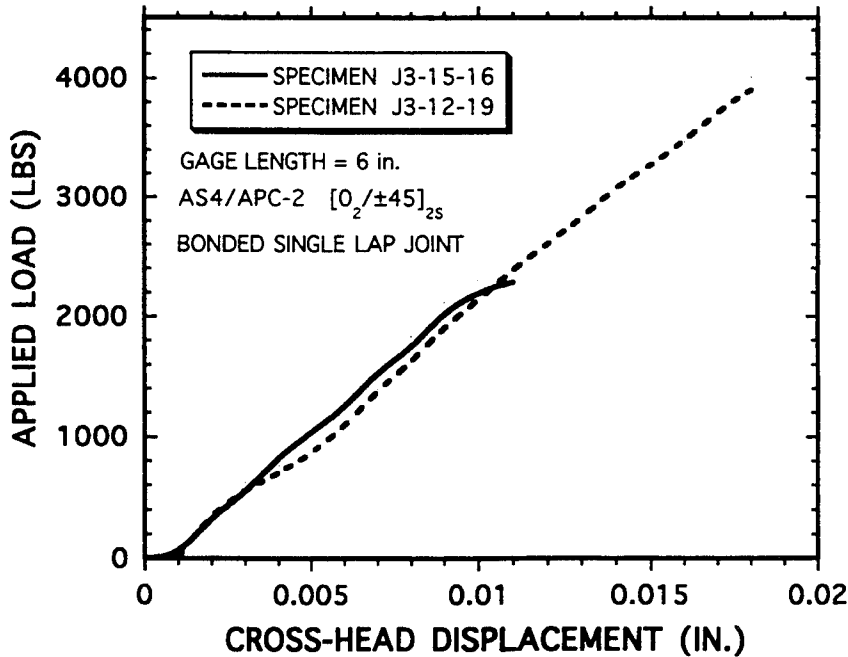


Figure 11. Load-crosshead deflection relations of AS4/APC-2 $[0_2/\pm 45]_{2s}$ laminates with bonded joints.

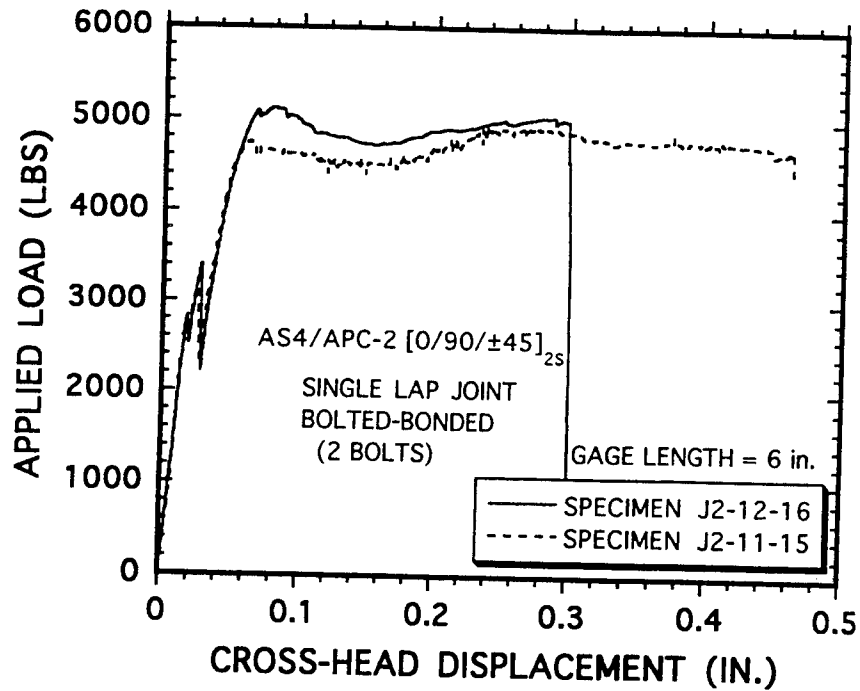


Figure 12. Load-crosshead deflection relations of AS4/APC-2 [0/90/±45]_{2s} laminates with bolted-bonded joints (2-bolt).

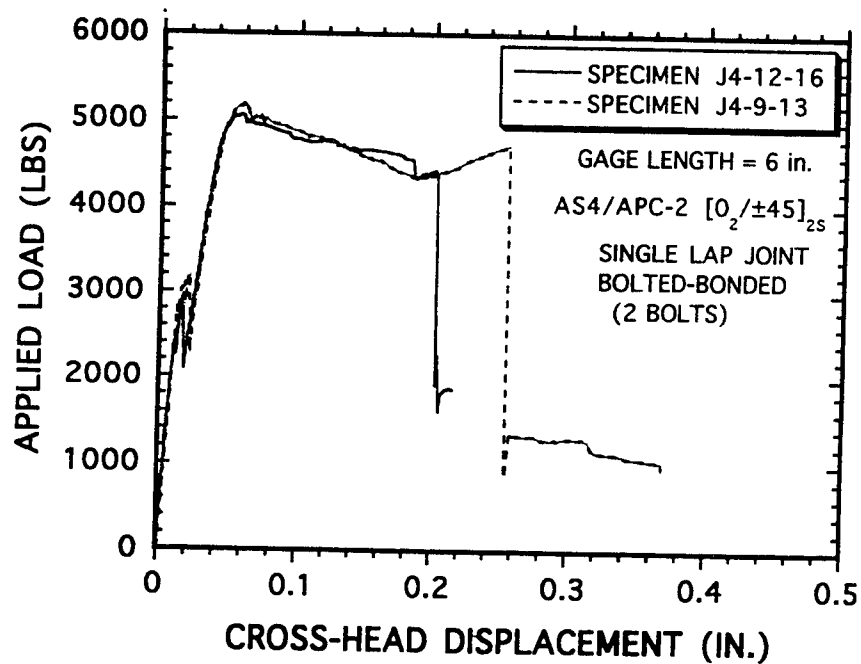


Figure 13. Load-crosshead deflection relations of AS4/APC-2 [0₂/±45]_{2s} laminates with bolted-bonded joints (2-bolt).

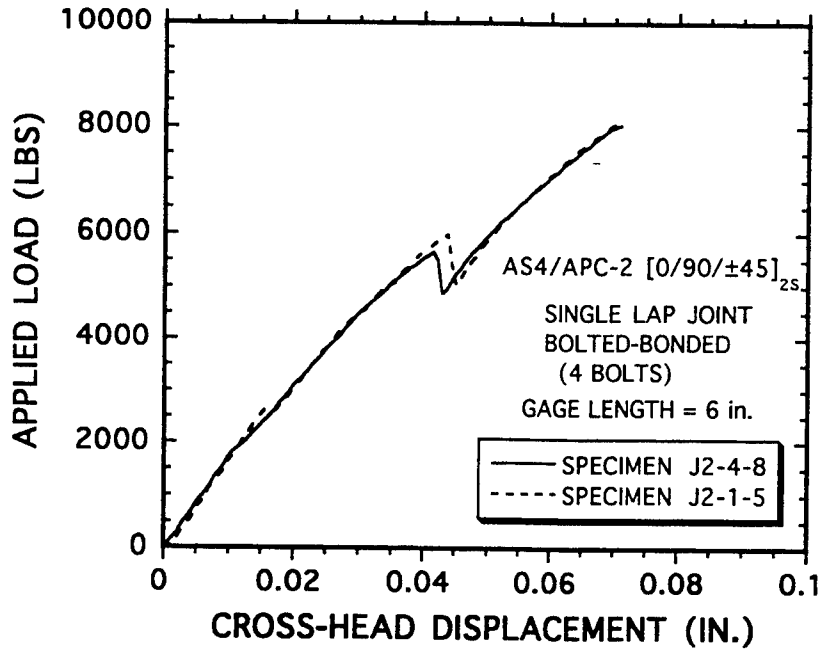


Figure 14. Load-crosshead deflection relations of AS4/APC-2 $[0/90/\pm 45]_{2s}$ laminates with bolted-bonded joints (4-bolt).

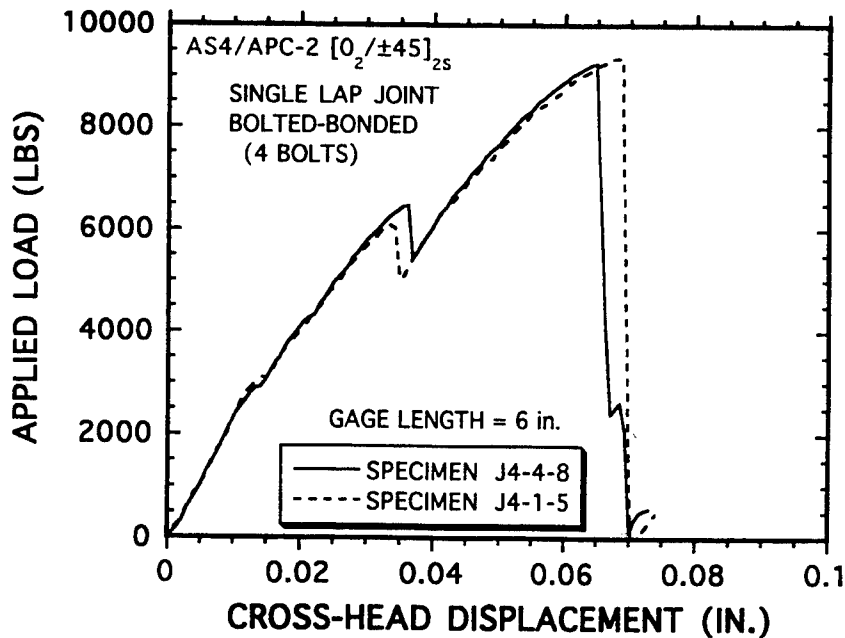


Figure 15. Load-crosshead deflection relations of AS4/APC-2 $[0_2/\pm 45]_{2s}$ laminates with bolted-bonded joints (4-bolt).

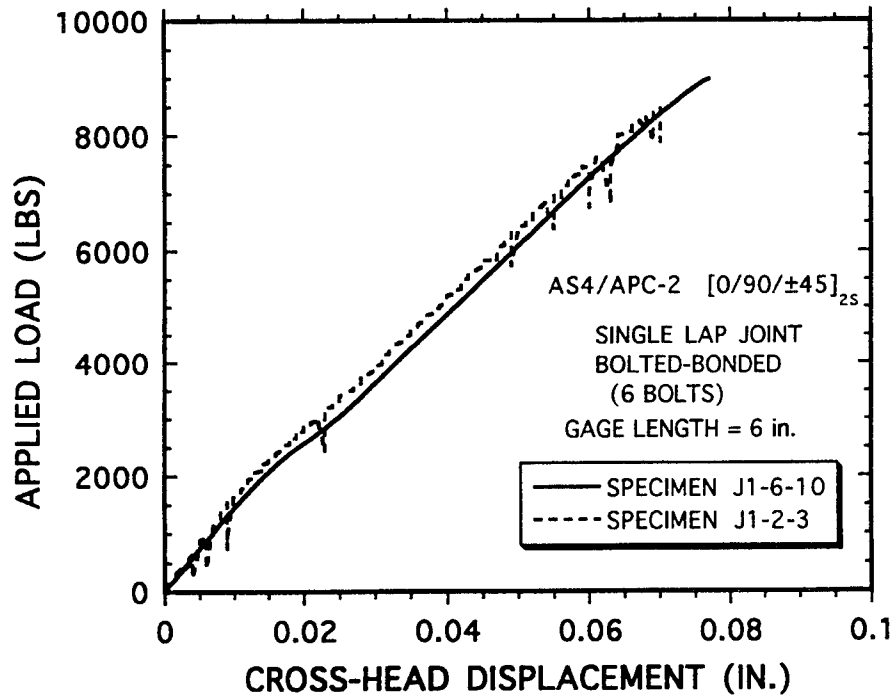


Figure 16. Load-crosshead deflection relations of AS4/APC-2 [0/90/±45]_{2s} laminates with bolted joints (6-bolt).

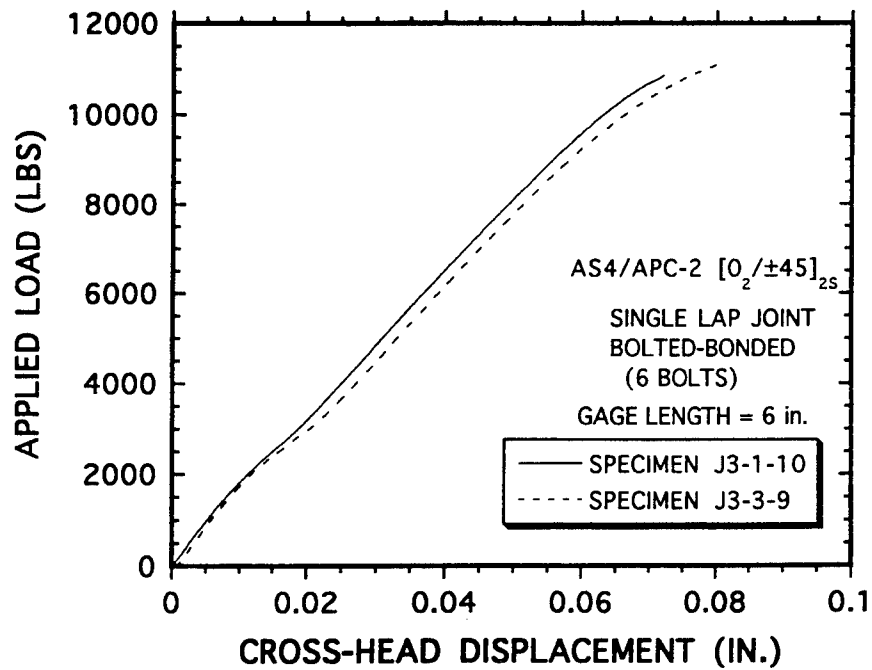


Figure 17. Load-crosshead deflection relations of AS4/APC-2 [0₂/±45]_{2s} laminates with bolted joints (6-bolt).

Table 1. Experimental results of Gr/PEEK AS4/APC-2 coupons.

SPECIMEN NUMBER	LAY-UP	MAX LOAD (lb)	STRENGTH (lb)	POISSON'S RATIO	LONGITUDINAL MODULUS (msi)
J1-21	[0/90/±45]2s	15000	81.5*	0.31	6.9
J1-22	"	16100	84.2	0.30	7
J1-23	"	15350	90.1	0.37	6.4
J1-24	"	15400	87.5		
J1-25	"	16500	84.0		
J1-26	"	16150	88.4		
AVERAGE		15750	86.8	0.33	6.7
STANDARD DEVIATION		581	3.9	0.04	0.32
J3-21	[0/0/±45]2s	26400	135	0.67	10.6
J3-22	"	24500	150	0.71	10.8
J3-23	"	27600	155	0.71	10.5
J3-24	"	26200	132		
J3-25	"	28800	134		
J3-26	"	29000	157		
AVERAGE		27083	144	0.70	10.6
STANDARD DEVIATION		1727	8.5	0.02	0.15

* : Torque applied to sample during set-up; not included in average.

Loading rate = 0.05 in/min

Gauge length of all specimens = 8.0 in

Table 2. Single lap shear strength (bonded joint) of Gr/PEEK AS4/APC-2 laminates.

SPECIMEN TYPE	SPECIMEN NUMBER	LAY-UP	MAX LOAD (lb)	SHEAR STRENGTH (psi)
BONDED	J1-11-19	[0/90/±45]2s	2263	447
	J1-12-20	"	2490	492
	J1-13-18	"	2500	494
	J1-14-17*	"	2011	397
	J1-15-16	"	3200	632
	AVERAGE:		2493	492
	STANDARD DEVIATION		992	303
	J3-11-20	[0/0/±45]2s	3300	652
	J3-12-19 [2]	"	4100	810
	J3-13-18	"	2500	494
	J3-14-17	"	3290	650
	J3-15-16**	"	2290	452
	AVERAGE:		3096	612
	STANDARD DEVIATION		1464	389

*: Bonded surfaces grit blasted, excluding in average.

** : Bonded surfaces sanded and grit blasted.

Gauge length of all specimens = 6 in

Loading rate = 0.05 in/min

Machine grip pressure = 2 ksi

If we consider only the specimens with their surfaces prepared by sanding method, the average shear strengths in the adhesive layers are 516 and 651 psi for the two layups. Table 3 lists the initial and complete debonding load, and bearing failure load of the specimens with bolted-bonded joints with a 2-bolt configuration. It also shows the complete debonding load and the ultimate failure load of the specimens with bolted-bonded joints with a 4-bolt configuration. The results of the specimens with bolted joints with a 6-bolt configuration are tabulated in Table 4.

4.3 Failure Mechanisms

The failure mechanisms of the $[0/90/\pm 45]_{2S}$ and the $[0_2/\pm 45]_{2S}$ laminates with bonded joints are practically the same. The failure initiates with laminate/adhesive debonding at one interface and jumps to the next interface, Figure 18.

Figures 19a-b show the front view and the edge view of the $[0/90/\pm 45]_{2S}$ specimen with bolted-bonded joints with a 2-bolt configuration after the ultimate failure. Complete debonding was observed in the adhesive layer. The corresponding results for a $[0_2/\pm 45]_{2S}$ laminate are illustrated in Figures 20a-b. The failure mechanisms involve bearing failure under the washer area and cleavage failure outside the washer area and a complete debonding between the laminate/adhesive interfaces.

Figures 21a-b illustrate a $[0/90/\pm 45]_{2S}$ specimen with bolted-bonded joints with a 4-bolt configuration after the ultimate failure. These pictures show a clean fracture across the interior row (from the free edge) of bolt holes and a complete laminate/adhesive interfacial debonding. The corresponding results for a $[0_2/\pm 45]_{2S}$ laminate, Figures 22a-b, show a zig-zag failure across the interior row of bolt holes and splitting and peeling in the outermost 0° layers. A complete interfacial debonding was observed between the laminate/adhesive interfaces.

A post-failure examination of the $[0/90/\pm 45]_{2S}$ specimens with bolted joints in a 6-bolt configuration reveals a failure plane occurring across the interior row of bolt holes, Figures 23a-b. There is a shift in failure locations (relative to the hole) from the region inside the washer to the region outside the washer. For the $[0_2/\pm 45]_{2S}$ specimens, Figures 24a-b, failure planes occur in a zig-zag pattern across the interior row of bolt holes with splitting and peeling in the outermost 0° layers.

Table 3. Strength of AS4/APC-2 specimens with bolted-bonded joints.

SPECIMEN TYPE	SPECIMEN NUMBER	LAY-UP	MAX LOAD (LB)	FAILURE* INITIATION (LB)	COMPLETE DEBONDING (LB)	
2-BOLT	J2-9-13	[0/90/±45]2s	4906	2840	3320	
	J2-10-14	"	**	2350	3280	
	J2-11-15	"	4896	2840	3350	
	J2-12-16	"	5127	2840	3410	
	AVERAGE:		4976	2718	3340	
	STANDARD DEVIATION		148	237	55	
	J4-9-13	[0/0/±45]2s	5200	2800	3200	
	J4-10-14	"	4990	3040	3100	
	J4-11-15	"	4900	3400	3615	
	J4-12-16	"	5010	2400	2800	
	AVERAGE:		5025	2910	3179	
	STANDARD DEVIATION		126	420	334	
	4-BOLT	J2-1-5	[0/90/±45]2s	8097		6010
		J2-2-6	"	8097		6205
J2-3-7		"	8097		5985	
J2-4-8		"	8097		5700	
AVERAGE:			8097		5975	
STANDARD DEVIATION			0		208	
J4-1-5		[0/0/±45]2s	9400		6195	
J4-2-6		"	9310		6200	
J4-3-7		"	9233		6690	
J4-4-8		"	9300		6575	
AVERAGE:			9311		6415	
STANDARD DEVIATION			69		256	

* : Failure initiation corresponds to first load drop of the load-deflection curve.

** : Specimen removed from test for observation.

Loading rate = 0.05 in/min

Gauge length of all specimens = 6.0 in

Table 4. Experimental results of AS4/APC-2 specimens with bolted joints (6-bolt).

SPECIMEN TYPE	SPECIMEN NUMBER	LAY-UP	MAX LOAD (LB)
6-BOLT	J1-1-4	[0/90/±45]2s	8220
	J1-2-3	"	8640
	J1-5-8	"	9100
	J1-6-10	"	8760
	J1-7-9	"	8860
	AVERAGE:		8716
	STANDARD DEVIATION		325
	J3-1-10	[0/0/±45]2s	10900
	J3-2-8	"	11125
	J3-3-9	"	11220
J3-4-7	"	11380	
J3-5-6	"	9300	
AVERAGE:		10785	
STANDARD DEVIATION		848	

Loading rate = 0.05 in/min
 Gauge length of all specimens = 6.0 in
 Machine grip pressure = 1000 psi

Table 5. Experimental results of AS4/APC-2 specimens with bolted joints (8-bolt).

SPECIMEN TYPE	SPECIMEN NUMBER	LAY-UP	MAX LOAD (LB)
8-BOLT	J1-12-20	[0/90/±45]2s	8019
	J1-14-17	"	8201
	AVERAGE		8110
	STANDARD DEVIATION		129
	J3-15-16	[0/0/±45]2s	9685
	J3-12-19	"	9784
J3-11-20	"	10272	
AVERAGE		9914	
STANDARD DEVIATION		298	

Loading rate = 0.05 in/min
 Gauge length of all specimens = 6.0 in
 Machine grip pressure = 1000 psi



Figure 18. Interfacial debonding of AS4/APC-2 specimens with bonded joints.

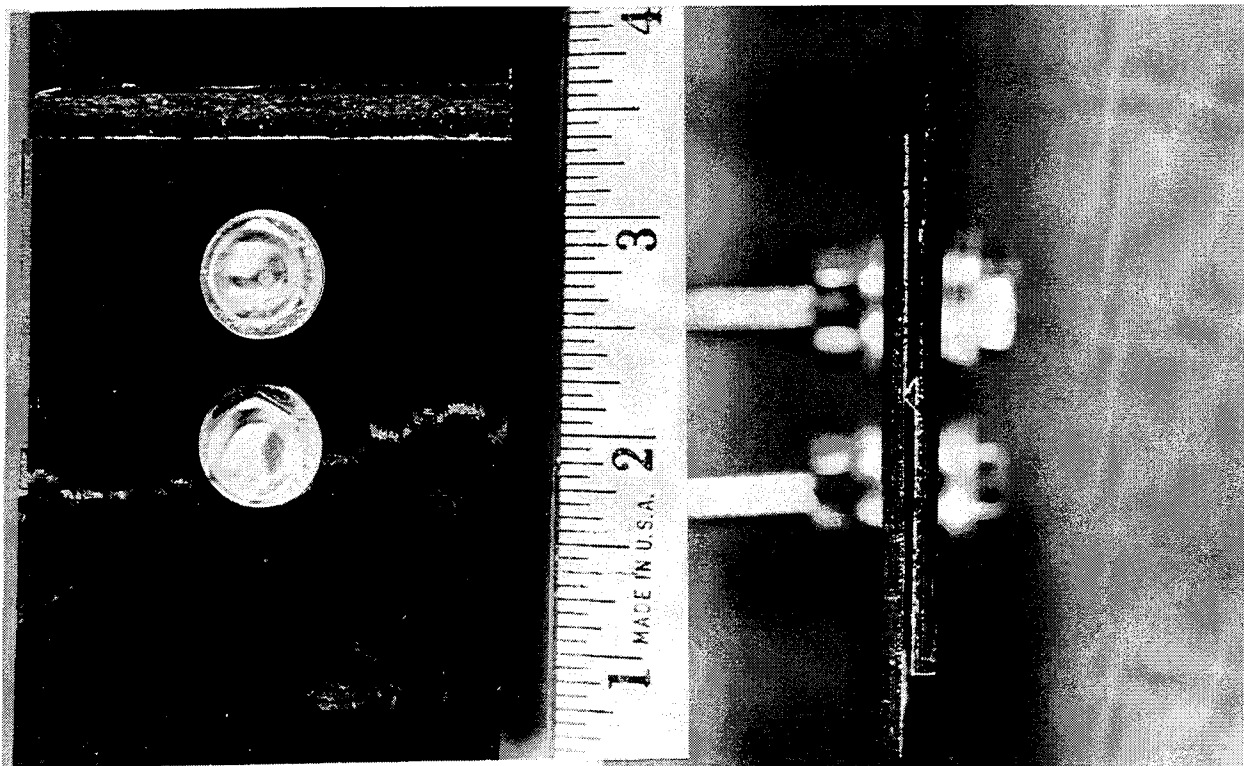


Figure 19. Failure mechanisms of an AS4/APC-2 $[0/90/\pm 45]_{2s}$ laminate with bolted-bonded joints (2-bolt).

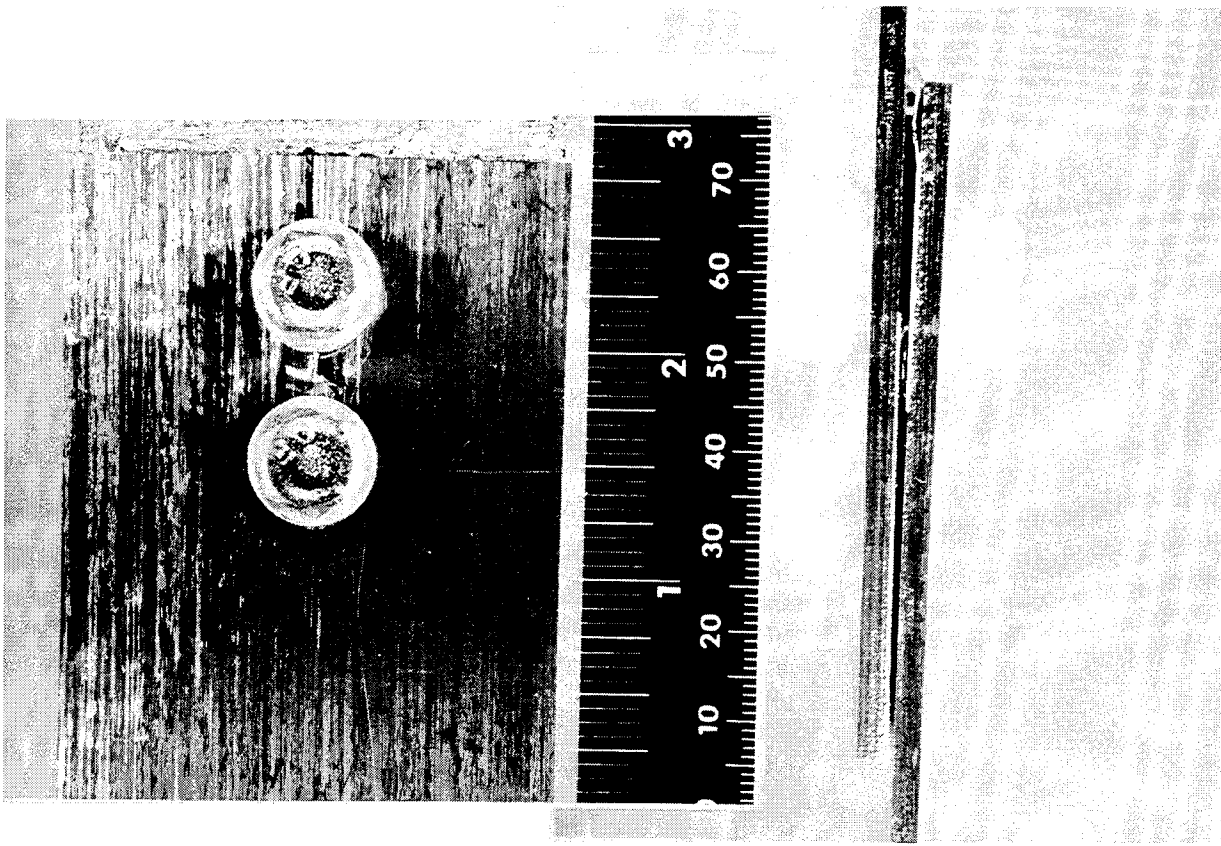


Figure 20. Failure mechanisms of an AS4/APC-2 $[0_2/\pm 45]_{2s}$ laminate with bolted-bonded joints (2-bolt).

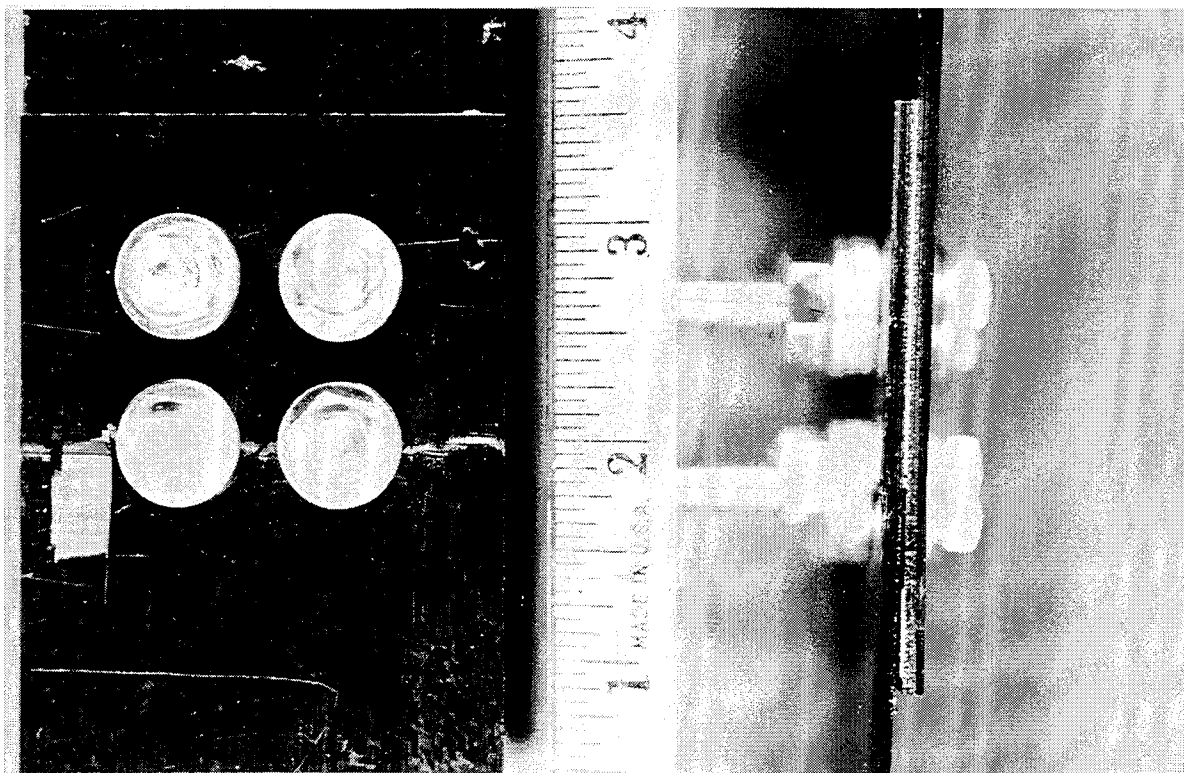


Figure 21. Failure mechanisms of an AS4/APC-2 $[0/90/\pm 45]_{2s}$ laminate with bolted-bonded joints (4-bolt).

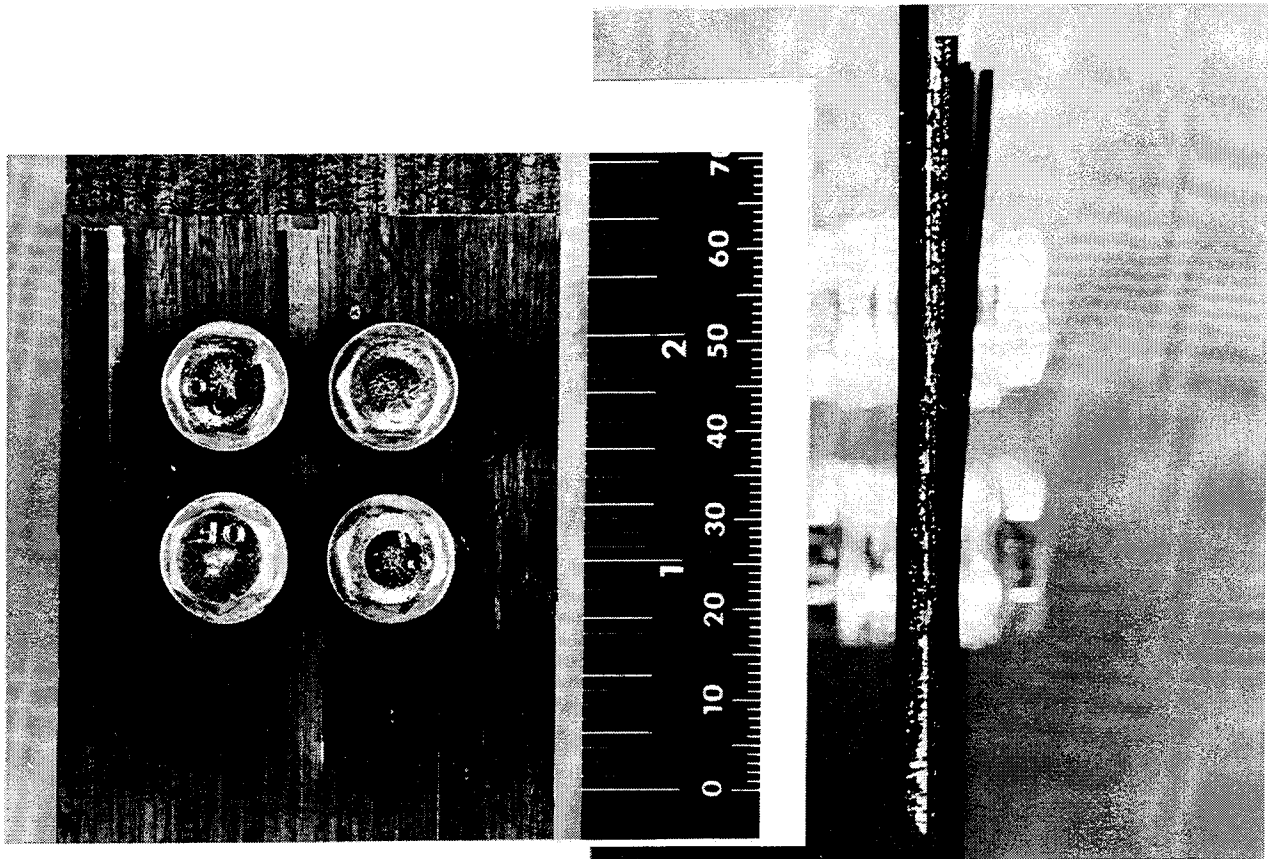


Figure 22. Failure mechanisms of an AS4/APC-2 $[0_2/\pm 45]_{2s}$ laminate with bolted-bonded joints (4-bolt).

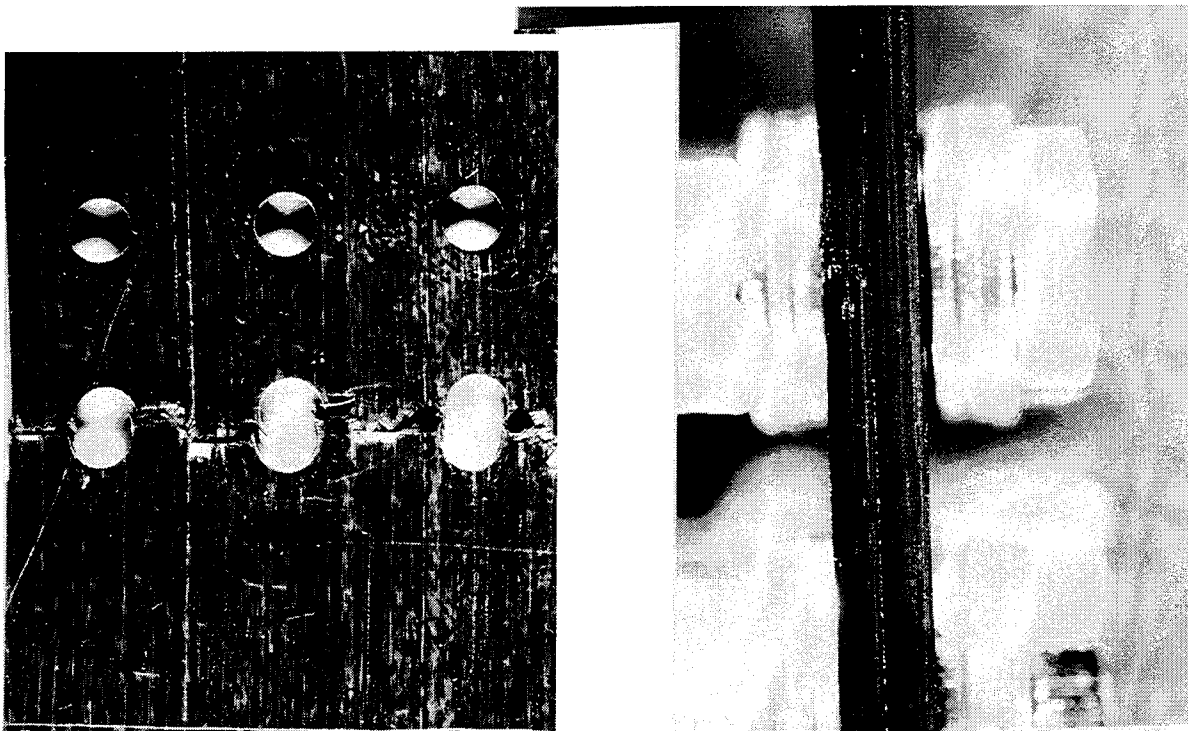


Figure 23. Failure mechanisms of an AS4/APC-2 $[0/90/\pm 45]_{2s}$ laminate with bolted joints (6-bolt).

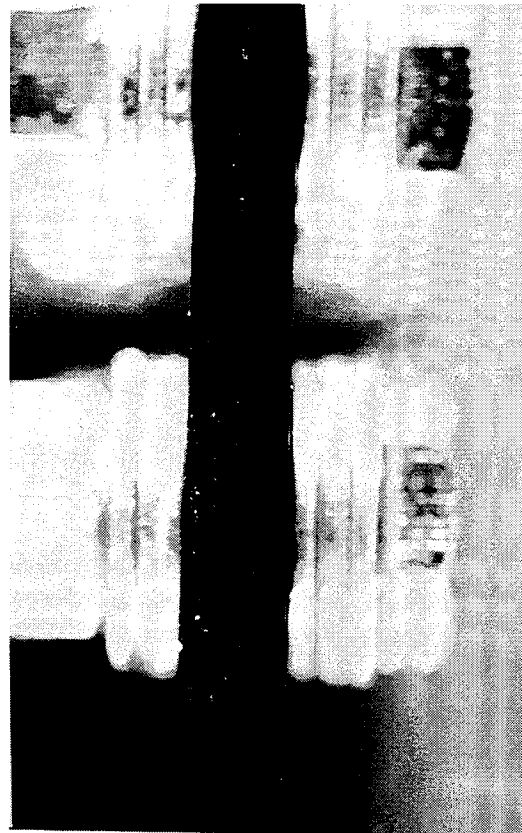
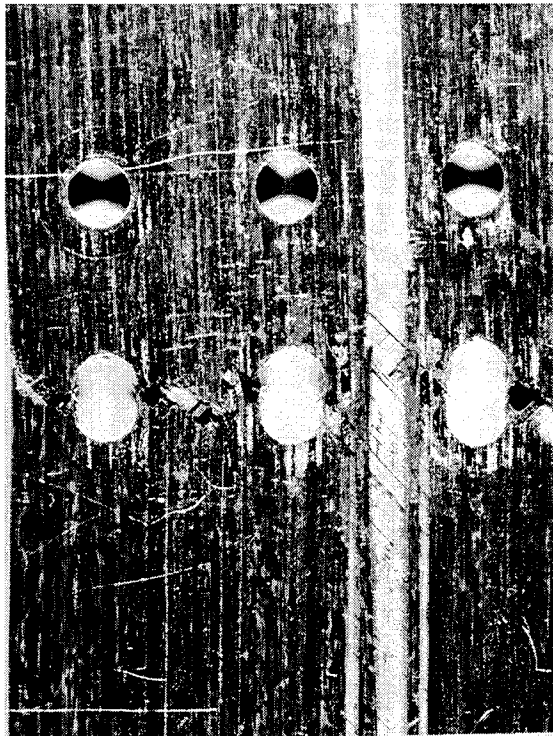


Figure 24. Failure mechanisms of an AS4/APC-2 $[0_2/\pm 45]_{2s}$ laminate with bolted joints (6-bolt).

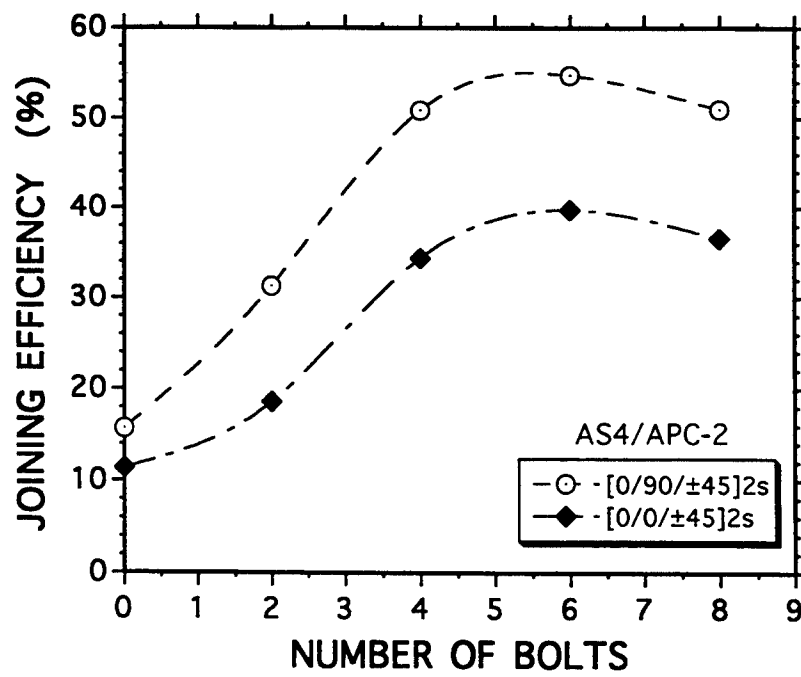


Figure 25. Joining efficiency versus number of bolts for AS4/APC-2 $[0/90/\pm 45]_{2s}$ and $[0_2/\pm 45]_{2s}$ laminates.

4.4 Efficiency of Single-lap Joints

Using the definition of joining efficiency defined in Section 2, we calculated the efficiency of the joining methods for the $[0/90/\pm 45]_{2S}$ and the $[0_2/\pm 45]_{2S}$ laminates with single-lap joint configurations. Figure 25 shows that the former layup has significantly higher joining efficiency than that of the later. The trends of these two curves for different layups are very consistent. Also in this figure, the data along the vertical line with zero number of bolts means bonded joints only. The data points with number of bolts equal to 2 and 4 are for bolted-bonded joints, and 6 and 8 are for bolted joints. When 1-bolt is used for bolted joint specimens the joining efficiencies are 13.7 and 7.9% for the $[0/90/\pm 45]_{2S}$ and the $[0_2/\pm 45]_{2S}$ layup, respectively. If we join the data points of each curve for N (number of bolts) $\neq 0$ they tend to approach the origin of the figure when $N = 0$. Both layups show that optimum joining efficiency of single-lap joint configurations can be achieved with N lies between 5 and 6. Adhesive layer does not affect the joining strength because it debonds completely much earlier than the ultimate failure.

5. Conclusion

Joining efficiency is one of the most important issues in the joining of composite structures. This experimental work shows that the highest efficiency for the graphite/PEEK AS4/APC-2 $[0/90/\pm 45]_{2S}$ and the $[0_2/\pm 45]_{2S}$ laminates with a single-lap joint configuration is 54.8 and 39.8%, respectively. The load level for complete debonding between the laminate/adhesive interfaces increases in bolted-bonded joined specimens with increasing number of bolts. However, since the debonding load is considerably lower than the ultimate failure load, adhesive bonding does not affect the ultimate load carrying capability. Before debonding occurs, adhesive joint increases the joint stiffness slightly compared to the bolted-joint specimen.

Joining efficiency for double-lap joints should be higher than that for single-lap joints because of the elimination of load eccentricity. Given the situation of a single-lap joint, the joining efficiency appears to be quite low and needs to be improved. We also conclude from this research that adhesive layer debonds at low stress level when peeling stress and out-of-plane shear stress are high in the adhesive layer of the thermoplastic composite (a common phenomenon in single-lap joints). Therefore, bolted joints should be considered favorably in single-lap joints and any other joint configurations where peeling stress and out-of-plane shear stress are high and tend to debond the adhesive layer.

6. References

1. S. J. Dastin, "Joining and Machining Techniques," Handbook of Composites, Ed., G. Lubin, Van Nostrand Reinhold Co., New York, 602-632 (1969).
2. L. J. Hart-Smith, "Bolted Joints in Graphite-Epoxy Composites," NASA-CR-144899 (June 1976).
3. D. L. Buchanan and S. P. Garbo, "Design of Highly Loaded Composite Joints and Attachment for Wing Structures," NADC-81194-60 (August 1981).
4. D. J. Watts, et al., "Development of Composites Technology for Joints and Cutouts in Fuselage Structure of Large Transport Aircraft," Semi-Annual Technical Report Number 1, ACEE-34-PR-3419 (October 1984).
5. S. J. Kong, "Conceptual Design of a High Load Transfer Mechanical Attachment for Tail Structures," NADC-81216-60 (August 1981).
6. S. W. Averill and H. R. Zamani, "Development of High Load Joints and Attachments for Composite Structure," NADC-81220-60 (August 1983).
7. R. L. Ramkumar, E. S. Saether and D. Cheng, "Design Guide for Bolted Joints in Composite Structures," Air Force Technical Report, AFWAL-TR-86-3035 (March 1986).
8. F. L. Matthews, "Bolted Joints," Composites Design, 4th edition, Chapter 18, S. W. Tsai, Ed., Think Composites (1988).
9. Olson, A. J and H. R. Pearson, "Complex Adhesive Bonded Assemblies," Symposium on Processing for Adhesives Bonded Structures at Stevens Institute of Technology, August 23-25, 1972.
10. Proceeding of Symposium for Processing of Adhesives Bonded Structures, Vols. I and II, Stevens Institute of Technology, August 23-25, 1972.
11. Horton, R. E., J. E. McCarty, et al., "Adhesive Bonded Aerospace Structures Standardized Repair Handbook," Air Force Technical Report AFML-TR-77-206, 1978.
12. Matthews, F. L., P. F. Kilty and E. W. Godwin, "A Review of the Strength of Joints in Fibre-Reinforced Plastics, Part 2. Adhesively Bonded Joints," Composites, January 1982, pp. 29-37.

13. Wegman, R. F., "Repair of Damage to Secondary Aircraft Structure of Advanced Composite Material," Plastic Report R51, October 1983.
14. Cochran, R. C., T. M. Donnellan, J. G. Williams, J. J. Katilaus and N. Nemeroff, "An Adhesive for Field Repair of Composites," Report No. NADC-88072-60, June 1988.
15. Hart-Smith, L. J., "Design Methodology for Bonded-Bolted Composite Joints Vol. I. Analysis Derivations and Illustrative Solutions," Air Force Technical Report AFWAL-TR-81-3154, June 1981.